

13A.5 APPLICATION OF DOPPLER RADAR DATA ASSIMILATION ON THE RETRIEVAL OF A MEI-YU FRONT WITHIN THE TAIWAN STRAIT ASSOCIATED WITH A HEAVY RAIN EVENT

Hsi-Chyi Yeh*

Aletheia University, Tamshui, Taipei, Taiwan

Abstract

With the incorporation of Doppler radar radial velocity by MM5/3DVAR system, a Mei-yu frontal system related to a coming heavy rain episode over southwestern Taiwan was retrieved within the Taiwan Strait on 6 June 2003. Significant frontal wind-shift (the prefrontal southwesterlies/the postfrontal northeasterlies) was reproduced over ocean, which was not captured by the NCEP reanalysis and the other datasets. Especially, the convectively induced strong wind ($>20 \text{ ms}^{-1}$) and mesoscale kinematic properties (horizontal convergence and cyclonic vorticity) were retrieved and enhanced along the surface frontal zone. Also, the orographically induced windward anticyclonic vorticity (ridge) and leeside cyclonic vorticity (trough) were reproduced over the southern Taiwan.

For the prediction of the heavy rainfall over southwestern Taiwan on 7 June 2003, the simulated rainfall distribution using Doppler radar data assimilation revealed a better performance.

1. Introduction

Over Taiwan, the Central Weather Bureau (CWB) classified heavy rain events into three new categories in 2004: A: $200 \text{ mm} > \text{daily rainfall} \geq 130 \text{ mm}$; B: $350 \text{ mm} > \text{daily rainfall} \geq 200 \text{ mm}$; C: $\text{daily rainfall} \geq 350 \text{ mm}$. During Taiwan Mei-yu season (mid-May to mid-June), localized heavy rain events with category A were frequently observed during the passage of the Mei-yu frontal system (Chen and Hui 1990; Trier et al. 1990; Ray et al. 1991; Li et al. 1997; Yeh and Chen 1998; Yeh et al. 2002; Yeh and Chen 2004) and the associated upper-level forcing (Li et al. 1997; and Yeh and Chen 2004) under the influence of island topography (Li et al. 1997; and Yeh and Chen 2002). However, the super heavy rain episode related to category C was not usual over Taiwan during Mei-yu season, but always caused badly damage

over mountainous regions associated with flash flooding and debris flow.

In this study, super heavy rainfall ($>350 \text{ mmday}^{-1}$) was observed over the southwestern Taiwan (Fig. 1) on 7 June 2003. The associated weather conditions were analyzed using surface observations, NCEP reanalysis data and local soundings. In addition, the Doppler radar data were incorporated into the initial field (NCEP-fnl data) to improve the analyses of the Mei-yu frontal system and the rainfall prediction for this super heavy rain event.

2. Weather Review

Based on surface analyses, a Mei-yu front had a weak thermal contrast and a slow moving southward. It reached the west of central Taiwan at 1200 UTC on 6 June and extended westward to southern China where the convection was active as shown from the satellite imagery (Fig. 2). Scattered rain showers were observed over Taiwan (not shown). Using the NCEP reanalyses data (Fig. 3), the daily mean on 6 June in the wind fields, geopotential height and specific

*Corresponding author address: Hsi-Chyi Yeh, School of General Education, Aletheia University, Tamshui, Taipei, Taiwan; E-mail: yehhc@email.au.edu.tw

humidity at 925-hPa and 500-hPa levels was analyzed respectively. At 925 hPa, a low pressure system with higher specific humidity ($16\text{-}19\text{ gg}^{-1}$) located over southern China. The strong wind ($>15\text{ ms}^{-1}$) over the South China Sea (SCS) was revealed. At 500 hPa, a relatively high specific humidity ($4\text{-}6\text{ gg}^{-1}$) zone passed through Taiwan area with strong westerly flow.

12-hr later, a low pressure system developed along the surface frontal zone over Taiwan and nearby ocean (Fig. 2), which was consistent with the coverage of the prevailed clouds. At 925 hPa (Fig. 3), the daily mean of geopotential height field also showed a low pressure system occurred over Taiwan area and southern China. The wind fields revealed the enhanced westerly flow over southern Taiwan and SCS instead of southerly or southwesterly flow there on 6 June. Also, the specific humidity ($16\text{-}19\text{ gg}^{-1}$) at this level increased over southern China, central-to-southern Taiwan and over the ocean east of Taiwan. At 500 hPa, the daily mean showed that a trough collocated with the low pressure system in low levels over Taiwan Strait. A high specific humidity zone also passed through Taiwan area on 7 June. These results revealed that the increased moisture content, the influence of the Mei-yu frontal system and an upper level trough provided favorable conditions to produce super heavy rainfall over southwestern Taiwan. During 8-9 June (Fig. 4), the high specific humidity zone dissipated as the low system in low levels moved northeastward. The decrease of moisture content was consistent with the reduction of the daily rainfall amount over Taiwan area during these two days.

To reveal the orographic effect on this super heavy rain event, the time series of a local sounding over southwestern Taiwan during 5-9 June were analyzed (Fig. 5). The wind profile and equivalent potential temperature (θ_e) revealed that the

environmental condition had a weak potential unstable below 2 km at 1200 UTC 6 June. During the super heavy rainy day (7 June), copious moist content in middle levels (3-7 km) was shown through the daytime with a weak potential unstable condition in low levels. During the nighttime, the moisture decreased in middle levels was significant. The localized moisture advection (wind component normal to island topography multiplied by the mixing ratio) revealed the maxima on 7 June (Fig. 6). It was consistent with the peak of 12-hr accumulated rainfall on 7 June (Fig. 7). This indicates that the orography is important in determining the temporal and spatial rainfall distributions over Taiwan.

3. 3DVAR for Doppler radial velocity

3.1. Procedures for Doppler wind 3DVAR

Four Doppler radar (Fig. 8) data over Taiwan were preprocessed using radar software developed by Deng (2002). The processing included that the ambiguity of the radar radial velocity was first removed before the data was interpolated in the vertical with 0.5 km interval under the terrain-following coordinate. To reduce the uncertainty of computational errors due to lots of data incorporated at the same time, only single layer at 1-km in height was chose to combine with the NCEP grid data (the first guess) at the same level.

Because of only wind speed available from the single Doppler radar, the optimal interpolation method was used to reanalyze the wind field using the radial wind speed and NCEP grid wind data at 1-km level within the horizontal scan domain ($\sim 200\text{ km}$) of each radar. Then, the reanalyzed wind field was assimilated with the first guess by MM5/3DVAR (Baker et al. 2004) system. The impact of the Doppler radar wind assimilation on the analyses and numerical simulations for a Mei-yu frontal system during a super heavy rain episode (7 June, 2003) was investigated.

3.2. Retrieval of a Mei-yu front

In the following numerical simulations, there are four domains with 135-km, 45-km, 15-km and 5-km horizontal resolution (Fig. 9), respectively. Under the limitation of the radar scan range (~230 km), three-dimensional variational data assimilation (3DVAR) was performed only in the nested 5-km domain.

In figure 10, the winds, relative vorticity, horizontal divergence, and sea-level pressure field at 925 hPa in the NCEP-fnl data was plotted. The cyclonic circulation and vorticity were revealed over Taiwan Strait and nearby the coast of southwestern Taiwan. It was associated with the low pressure system along the Mei-yu frontal zone. However, the wind shift (prefrontal northeasterlies and postfrontal southwesterlies) and frontal convergence zone was not illustrated (Fig. 10).

With incorporation of Doppler radial winds, the wind shift along the Mei-yu frontal zone was retrieved within the Taiwan Strait (Fig. 11). Convectively induced strong winds ($>20 \text{ ms}^{-1}$), and the deceleration and deflection of the airflow due to the island topography of Taiwan were also illustrated at 925 hPa. The cyclonic vorticity and horizontal convergence along the surface frontal zone was enhanced. The windward anticyclonic vorticity and leeside cyclonic vorticity due to the orographic effect was shown over the southern Taiwan (Fig. 11). These results indicate that data assimilation of the radar radial velocity reasonably retrieved and enhanced the kinematic properties of the Mei-yu front. Also, the effect of island topography on the approaching airflow was revealed.

4. Numerical simulation

A primary approach to assimilate the unconventional data into the initial condition of the numerical simulation is to improve the initial fields and the associated weather forecasting, especially in the

rainfall amount and distribution. In this study, MM5/3DVAR was conducted to perform the data assimilation and numerical simulations.

Recall that the surface frontal kinematic properties was retrieved and enhanced within the Taiwan Strait. Thus, the improvement in the prediction of rainfall amount and distribution by assimilation of radar radial velocity through comparing the NCEP-fnl and 3DVAR experiments was shown in Figure 12.

Without data assimilation, the simulated rainfall amount and distribution over Taiwan area on 7 June, 2003 by NCEP-fnl run was not good. Most of rainfall was simulated over the nearby ocean of Taiwan. In contrast, the experiment of 3DVAR showed that the simulated rainfall amount ($>300 \text{ mmday}^{-1}$) and distribution (Fig. 12) over southwestern Taiwan was better than that in the NCEP-fnl experiment. Although the rainfall over southwestern Taiwan was reproduced in the 3DVAR run, the result still had some discrepancies from the observations. Recall that only single level (1-km) radar radial velocity was assimilated into the initial condition. Therefore, further studies are needed to weather forecasting using unconventional dataset.

5. Summary

In this super heavy rain event ($>350 \text{ mmday}^{-1}$) on 7 June 2003, the NCEP reanalyses revealed that the increased moisture content, the influence of the Mei-yu frontal system and an upper level trough provided favorable conditions to produce super heavy rainfall over southwestern Taiwan. Localized moisture advection (wind component normal to island topography multiplied by the mixing ratio) revealed the maxima on 7 June based on the time series of a sounding over southwestern of Taiwan. It was consistent with the peak of 12-hr accumulated rainfall there. This indicates that the orography is also important in determining the temporal and spatial

rainfall distributions over Taiwan.

With incorporation of Doppler radial winds, the wind shift along the Mei-yu frontal zone was retrieved within the Taiwan Strait. Convective-induced strong winds ($>20 \text{ ms}^{-1}$), and the deceleration and deflection of the airflow due to the island topography of Taiwan were also illustrated at 925 hPa. The cyclonic vorticity and horizontal convergence along the surface frontal zone was enhanced. In addition, the simulated rainfall amount ($>300 \text{ mmday}^{-1}$) and distribution (Fig. 12) over southwestern Taiwan in the experiment with radar data assimilation was better than that in the NCEP-fnl experiment.

Acknowledgments

Thanks for MMM Division, National Center for Atmospheric Research to provide the MM5 3D-VAR data assimilation system, and Taiwan Central Weather Bureau to provide the Doppler radar data. This research was supported by the National Science Council of the ROC under Grant NSC 93-2625-Z-156-001 and NSC 94-2625-Z-156-001

References

Barker, D. M., W. Huang, Y. -R. Kuo, J. Bourgeois, and Q. N. Xiao, 2004: A three-dimensional variational data assimilation system for MM5: Implementation and initial results. *Mon. Wea. Rev.*, **132**, 897–914.

- Chen, Y. -L., and N. B. -F. Hui, 1990: Analysis of a shallow front during the Taiwan Area Mesoscale Experiment. *Mon. Wea. Rev.*, **118**, 2649–2667.
- Li, J., Y.-L. Chen, and W.-C. Lee, 1997: Analysis of a heavy rainfall event during TAMEX. *Mon. Wea. Rev.*, **125**, 1060–1081.
- Ray, P.-S., A. Robinson, and Y. Lin, 1991: Radar analysis of a TAMEX frontal system. *Mon. Wea. Rev.*, **119**, 2519–2539.
- Trier, S. B., D. B. Parsons, and T. J. Matejka, 1990: Observations of a subtropical cold front in a region of complex terrain. *Mon. Wea. Rev.*, **118**, 2449–2470.
- Yeh, H. -C., and Y. -L. Chen, 1998: Characteristics of rainfall distribution over Taiwan during TAMEX. *J. Appl. Meteor.*, **37**, 1457–1469.
- _____, and _____, 2002: The role of offshore convergence on coastal rainfall during TAMEX IOP 3. *Mon. Wea. Rev.*, **130**, 2709–2730.
- Yeh, H. -C., T. -J. G. Chen, 2004: Case study of an unusual heavy rainfall event over Eastern Taiwan during the Mei-Yu Season. *Mon. Wea. Rev.* **132**, 320-337.
- _____, G. T. -J. Chen, and W. T. Liu, 2002: Kinematic characteristics of a Meiyu front detected by the QuikSCAT oceanic winds. *Mon. Wea. Rev.*, **130**, 700–711.

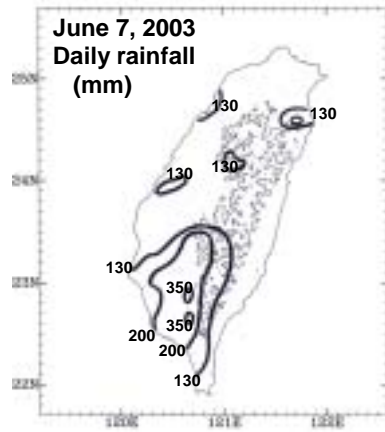


Fig. 1. Daily rainfall on June 7, 2003.

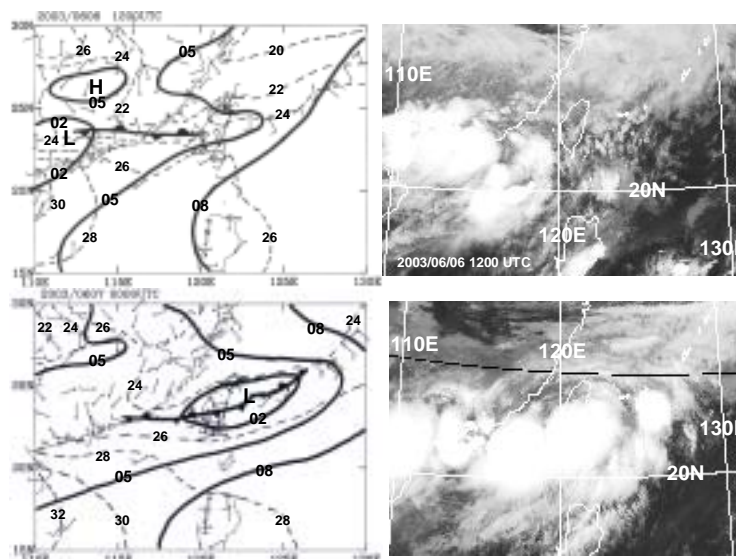


Fig. 2. Surface analyses and satellite imageries on 1200UTC June 6 and 0000UTC June 7, 2003.

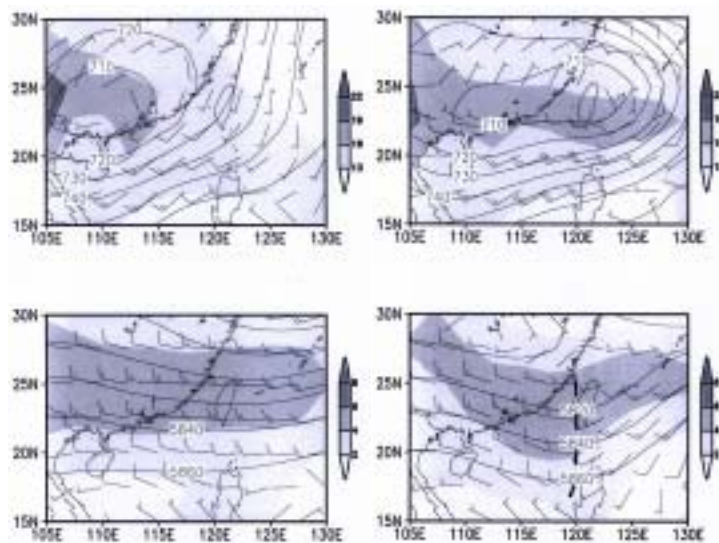


Fig. 3. Wind fields and specific humidity at 925 hPa & 500 hPa on June 6 and 7, 2003. full barb: 10 ms⁻¹. Half barb: 5 ms⁻¹. Specific humidity (g/g) is shaded

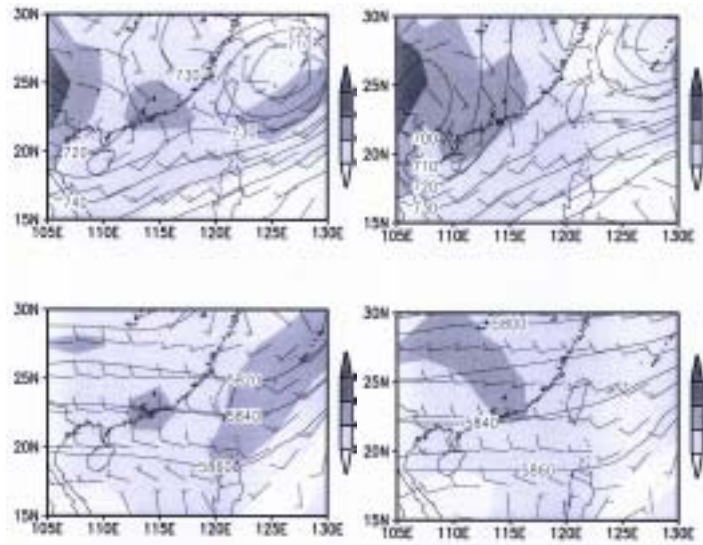


Fig. 4. Wind fields and specific humidity at 925 hPa & 500 hPa on June 8 and 9, 2003. full barb: 10 ms⁻¹. Half barb: 5 ms⁻¹. Specific humidity (g/g) is shaded

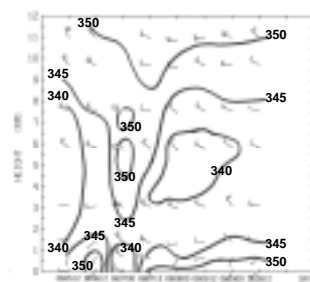


Fig. 5. Time series of soundings at 46750 with wind field and equivalent potential temperature during 5-9 June, 2003. Full barb: 10 ms⁻¹. Half barb: 5 ms⁻¹.

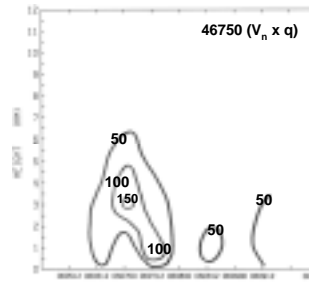


Fig. 6. Localized moisture advection at 46750 during 5-9 June, 2003.

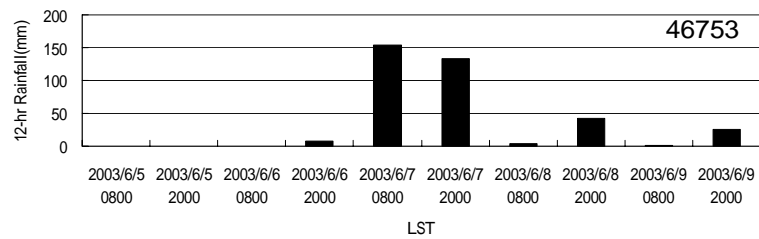


Fig. 7. 12-hr accumulated rainfall at 46753 during 5-9 June, 2003.

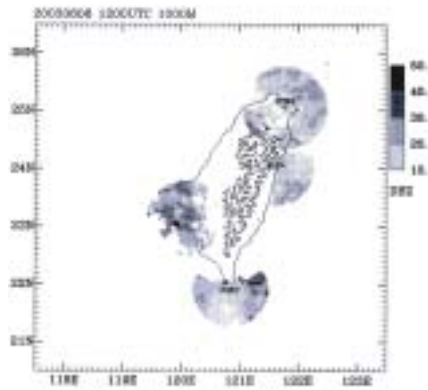


Fig. 8. Radar reflectivity at RCWF, RCCG, RCKT and RCHL at 1200UTC 6 June, 2003.

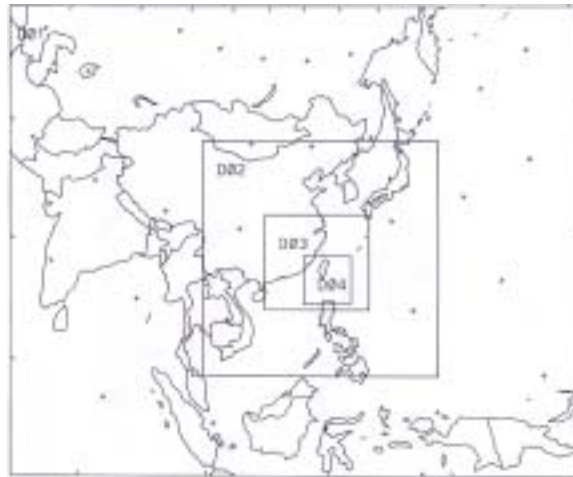


Fig. 9. Model Domains. D1: 135 km, D2: 45 km, D3: 15 km and D4: 5 km

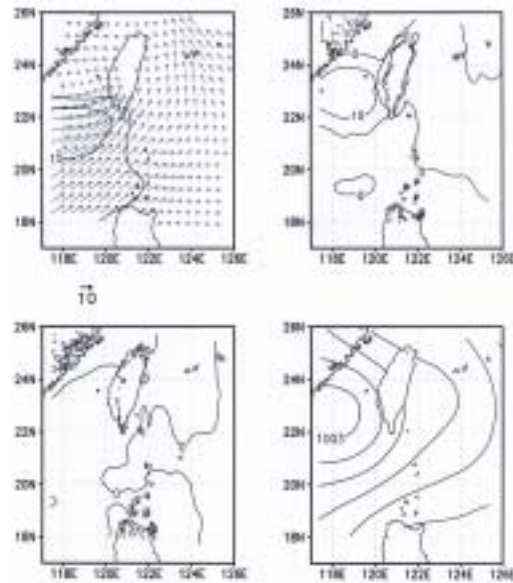


Fig. 10. NCEP-fnl data with wind vector, relative vorticity, divergence and sea level pressure field at 1-km level at 1200 UTC on 6 June, 2003.

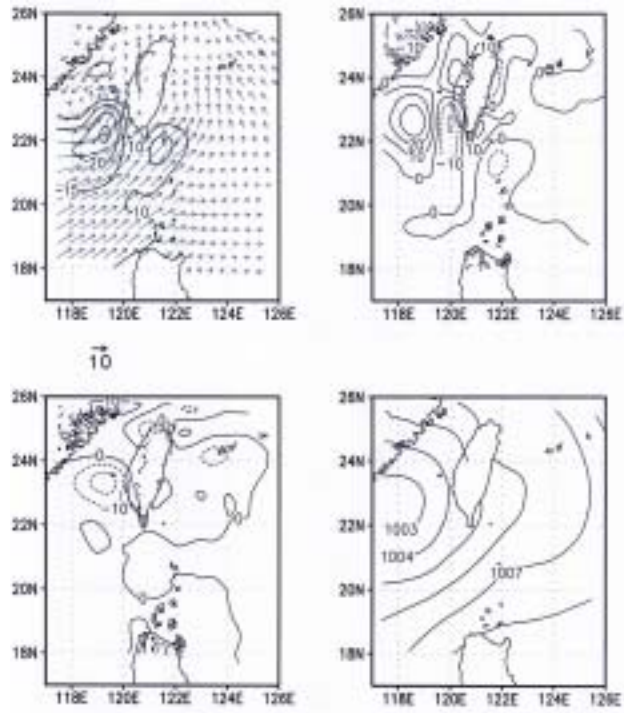


Fig. 11. Wind vector, relative vorticity, divergence and sea level pressure field by the 3DVAR of Doppler radial winds at 1-km level at 1200 UTC on 6 June, 2003.

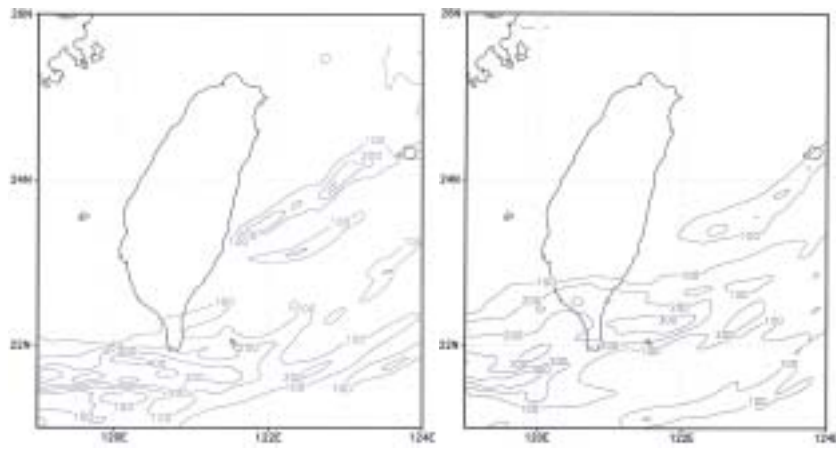


Fig. 12. Simulated rainfall distributions by NCEP and 3DVAR experiments on 7 June, 2003.